Coherent Manipulation of Electron Spins in the {Cu_{3}} Spin Triangle Complex Impregnated in Nanoporous Silicon

K.-Y. Choi, Z. Wang, H. Nojiri, J. van Tol, P. Kumar, P. Lemmens, B. S. Bassil, U. Kortz, and N. S. Dalal

Phys. Rev. Lett. **108**, 067206 — Published 10 February 2012

DOI: 10.1103/PhysRevLett.108.067206

Coherent Manipulation of Electron Spins in the {Cu_3} Spin Triangle Complex Impregnated in Nanoporous Silicon

K.-Y. Choi,[1,*] Z. X. Wang,[2] H. Nojiri,[3] J. van Tol,[2] P. Kumar,[4]
P. Lemmens,[4] B. S. Bassil,[5] U. Kortz,[5] and N. S. Dalal[2]

[1]*Department of Physics, Chung-Ang University,*
221 Huksuk-Dong, Seoul 156-756, Republic of Korea
[2]*Department of Chemistry and Biochemistry,*
Florida State University and National High Magnetic Field Laboratory,
Tallahassee, Florida 32306-4390, USA
[3]*Institute for Materials Research, Tohoku University,*
Katahira 2-1-1, Sendai 980-8577, Japan
[4]*Institute for Condensed Matter Physics,*
TU Braunschweig, D-38106 Braunschweig, Germany
[5]*School of Engineering and Science, Jacobs University,*
P.O. Box 750 561, 28725 Bremen, Germany

Abstract

We report on coherent manipulation of electron spins in an antiferromagnetically coupled spin triangle {Cu_3-X} (X=As, Sb) impregnated in free standing nanoporous silicon (NS) by using 240 GHz microwave pulses. Rabi oscillations are observed and the spin coherence time is found to be T_2 = 1066 ns at 1.5 K. This demonstrates that the {Cu_3-X}:NS hybrid material provides a promising scheme for implementing spin-based quantum gates. By measuring the spin relaxation times of samples with different symmetries and environments we give evidence that a spin chirality is the main decoherence source of spin triangle molecules.

In recent years, the possibility of employing electron spins in solid-state systems as essential ingredients of quantum devices and computers has been vigorously pursued and tested[1]. Among several proposed schemes molecular magnets are considered as promising candidates for the realization of spin-based qubits and quantum gates[2–8]. The entangled quantum state can be generated by (i) radiating microwave pulses with a frequency corresponding to the energy difference between the discrete levels[9,10], and/or (ii) introducing a tunable coupling between well-defined molecular clusters[11].

In several molecular magnets (for example, $\{Cr_7Ni\}$, $\{V_{15}\}$, $\{Fe_3\}$, $\{Fe_4\}$, and $\{Fe_8\}$) coherence times were measured to be several hundreds of nanoseconds and coherent manipulation of electron spins was demonstrated by means of pulsed electron paramagnetic resonance (EPR) [12–17]. In spite of their success as a single qubit, however, most of works have been performed in a frozen solution to limit strong spin decoherence arising from intermolecular dipolar interactions. This makes it difficult to scale these systems to larger register sizes[18] and therefore requires an alternative scheme, in which an array of coupled molecular clusters is embedded in a microwave cavity.

An alternating sequence of two different isosceles antiferromagnetic (AF) spin triangles has been proposed for molecule-based quantum gates[19]. Without invoking a fine tuning of intermolecular interactions exchange interactions between two triangles can be selectively switched on by exciting one of triangles to excited states. This motivates us to examine the spin triangle cluster $Na_{12}[X_2W_{18}Cu_3O_66(H_2O)_3]\cdot 32H_2O$ [abbreviated as $\{Cu_3\text{-}X\}$ (X=As,Sb)], known for pronounced spin chirality effects[20,21]. For the realization of scalable quibts, we first settle the question about additional decoherence sources, which might arise when the $\{Cu_3\text{-}X\}$ molecules are integrated to semiconducting nano-structures. Free standing nanoporous silicon (NS) could serve as a test bed to address such decoherence mechanisms due to ease of fabrications. In this paper, we report on the successful incorporation of $\{Cu_3\text{-}X\}$ in NS [See Fig. 1 (a)] as well as on the first experimental observation of a coherent manipulation of electron spins in $\{Cu_3\}$:NS complex by using pulsed 240 GHz EPR spectroscopy. Our results show that a new type of a hybrid material $\{Cu_3\}$:NS can provide a prospective avenue towards the design of electron spin based quantum gates.

NS layers were prepared by electrochemical anodic etching of highly doped, p^+-type (100)-oriented silicon substrates with a resistivity of $0.01 - 0.02\ \Omega$cm[22,23]. The pore diameter and porosity of oxidized NS are of the order of 5-10 nm and 40 %, respectively. Aqueous solutions

of the {Cu_3-X} molecules were dropped onto the oxidized NS and then we waited for 5-6 h until the molecules are adsorbed by the porous matrix. {Cu_3-X}:NS was rinsed with distilled water to remove the residual material on the NS surface. Here we remark that there is no possibility of oxygen adsorption in NS because the thermally annealed NS is immediately immersed in a {Cu_3-X} solution and the {Cu_3-X} solution itself contains oxygen neither in an ionic nor in a free form. The {Cu_3-X} molecules are oriented vertically within NS since a diameter of the NS fits well with a molecule size. For measurements we use large amounts of {Cu_3}:NS layers, which are randomly oriented.

Magnetic susceptibility was measured by using a SQUID magnetometer (Quantum Design MPMS) over $1.8 - 200$ K at H=1000 Oe. Magnetization measurements were carried out by means of a standard inductive method using compensated pickup coils and a pulse magnet[24]. 240 GHz continuous wave (cw)- and pulsed EPR experiments were performed on a home-built superheterodyne high field instrument[25].

The spin Hamiltonian of {Cu_3-X} is given by

$$\mathcal{H} = \sum_{i=1}^{3} \mathbf{J}_{i\,i+1}\mathbf{S}_i \cdot \mathbf{S}_{i+1} + \sum_{i=1}^{3} \mathbf{D}_{i\,i+1} \cdot [\mathbf{S}_i \times \mathbf{S}_{i+1}] + \mu_B \sum_{i=1}^{3} \mathbf{S}_i \cdot \tilde{\mathbf{g}}_{i\,i} \cdot \mathbf{H}_i, \qquad (1)$$

where the exchange coupling constants, $\mathbf{J}_{i\,i+1}$, the Dzyaloshinsky-Moriya (DM) vectors, $\mathbf{D}_{i\,i+1}$, and the g-tensors, $\tilde{\mathbf{g}}_{i\,i}$, are defined as a site-dependent quantity with a periodic boundary condition. For the crystals the magnetic parameters are listed in Table I.

The temperature dependence of the magnetic susceptibility, $\chi(T)$ of the {Cu_3-As}:NS agrees with that of the bulk {Cu_3-As} [Compare the open square and the solid line in Fig. 1(b)]. This indicates that the ground state spin and the electronic structure of the {Cu_3-X} molecules are hardly affected by chemical interactions between the molecules and the NS walls. This might be due to the fact that the core electron spins are well secured by peripheral ligands. Compared to the crystal, the magnetization steps of the {Cu_3-As}:NS

TABLE I: A list of the magnetic parameters of the {Cu_3-X}(X=As, Sb) compounds. The subscripts denote a site of copper spins and the superscripts are a component of the magnetic parameters.

	$J_{12}^{x,y}$	J_{12}^{z}	$J_{23}^{x,y} = J_{31}^{x,y}$	$J_{23}^{z} = J_{31}^{z}$	$D_{i\,i+1}^{z}$	$D_{12}^{x,y}$	$g_{11}^{x,y}$	$g_{22}^{x,y}$	$g_{33}^{x,y}$	g_{ii}^{z}
{Cu_3-As}	4.50 K	4.56 K	4.03 K	4.06 K	0.53 K	0.53 K	2.25	2.10	2.40	2.06
{Cu_3-Sb}	4.49 K	4.54 K	3.91 K	3.96 K	0.52 K	0.52 K	2.24	2.11	2.40	2.07

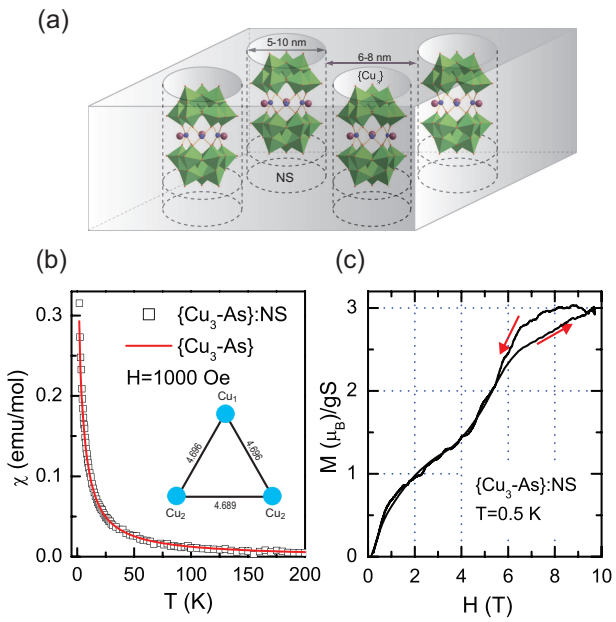

FIG. 1: (a) A sketch of a single NS layer enclosing $\{Cu_3\text{-X}\}$ molecular clusters. A pore diameter is an order of 5-10 nm and a distance between pores is of 6-8 nm. Color codes: Cu(II), blue; Na, plum; O, red. The rest atoms are hidden for clarity. (b) Comparison of temperature dependence of the magnetic susceptibility between the $\{Cu_3\text{-As}\}$:NS (open square) and the $\{Cu_3\text{-As}\}$ bulk (solid line) measured at H=1000 Oe. Inset: isosceles spin triangle with distances Cu_1-Cu_2=4.696 Å and Cu_2-Cu_2=4.689 Å. (c) Magnetization curve versus pulsed magnetic field at T=0.5 K. The saturated magnetization is normalized by gS with a g-factor and a spin S=1/2.

complexes are less pronounced [compare Fig. 1(c) and Fig. 2 of Ref.17]. This is partly ascribed to angle-averaged effects since the measurements were performed on an ensemble of randomly oriented molecules. In addition, thermal heating effects should be also taken into account because the measured temperature is a little bit high for $\{Cu_3\text{-As}\}$:NS.

Figure 2(a) shows the field-swept EPR spectrum recorded by integrating a spin echo signal at 1.5 K and $\nu = 240$ GHz for the $\{Cu_3\text{-As}\}$:NS. The spectrum is spread over the wide field range of 6-10 T while showing powder-shape absorption curves because molecules with different field orientations are excited at different resonance fields. Thanks to the enhanced sensitivity in a cw mode, we were able to measure the cw ESR spectrum with fewer amounts of aligned NS layers at 5 K. This yields single crystal-like sharp peaks with the field direction perpendicular to a triangle plane. This confirms that the $\{Cu_3\text{-X}\}$ molecules within NS is oriented vertically. The strongest cw peak at 7.55 T is assigned to the transition **1**(**1'**) from

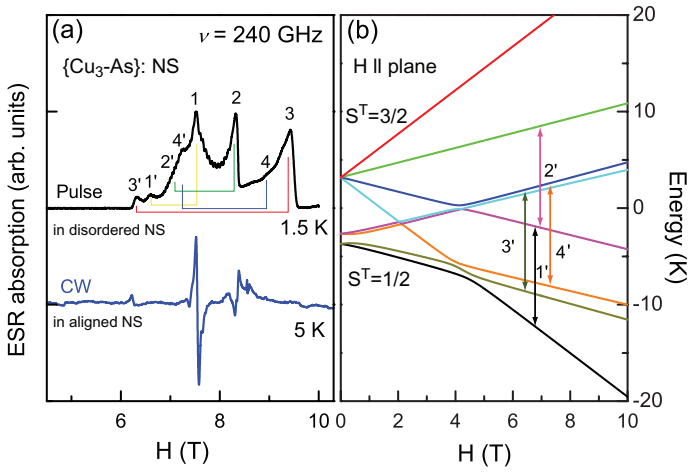

FIG. 2: (a) A spin echo signal of {Cu_3-As}:NS as a function of an external field at T=1.5 K and derivative of the cw EPR absorption versus external field measured at 240 GHz and 5 K. (b) Energy level diagram for an external field parallel to a spin triangle plane (H ∥ plane) determined by the Hamiltonian Eq. (1) and the magnetic parameters listed in Table I. The prime (unprimed) numbers and arrows indicate the observed EPR transitions between energy levels for H ∥ (H ⊥) plane.

the ground state, that is, $|\frac{3}{2};-\frac{3}{2}\rangle \rightarrow |\frac{3}{2};-\frac{1}{2}\rangle$ [see Fig. 2(b)]. The next strong peak at 8.35 T corresponds to the transition **2**(**2'**) from the excited $S^T = 3/2$ state: $|\frac{3}{2};-\frac{1}{2}\rangle \rightarrow |\frac{3}{2};\frac{1}{2}\rangle$. The weak signals around 6.3 T and 9.5 T originate from the transitions **3**(**3'**) and **4**(**4'**) between the $S^T = 1/2$ levels. We note that the spin-echo signals of the $S^T = 1/2$ levels are very broad as the mixing degree of the spin chiral states depends strongly on the components of the DM vectors and thus the resonance fields vary strongly with the orientation.

The upper panel of Fig. 3 shows the decay curve due to spin-lattice relaxation time T_1 process, measured for {Cu_3-As}:NS by using an inversion recovery pulse sequence (π-τ_1-π/2-τ_2-π-τ_2-echo) with varying τ_1 and fixed $\tau_2 = 300$ ns at T=1.5 K and H=7.63 T. We try to fit the echo decay curve by (i) a single exponential function, $I = A\exp(-T/T_1)$ with $T_1 = 54.8\ \mu s$, and (ii) a double exponential function, $I = A\exp(-T/T_{long}) + B\exp(-T/T_{short})$ with $T_{short} = 27.8\ \mu s$ and $T_{long} = 301\ \mu s$. The latter gives a better description. The short T_1 might arise from a strong spectral diffusion because the microwave pulses excite a small portion of the whole spectrum due to the limited excitation bandwidth. In contrast, T_{long} presents the spin-lattice relaxation time T_1.

The inset of Fig. 3 shows the intensity of Hahn echoes (π/2-τ-π-τ-echo) measured for the

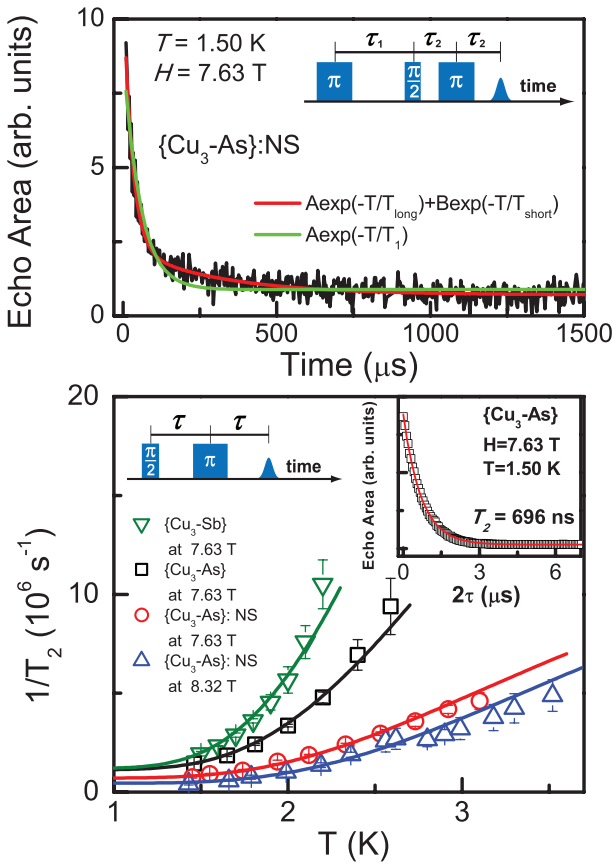

FIG. 3: (Upper panel) Echo decay measured for {Cu$_3$-As}:NS by a recovery pulse sequence at T=1.50 K and H=7.63 T. The red solid line is a fit to a double exponential function, $I = A\exp(-T/T_{long}) + B\exp(-T/T_{short})$ with $T_{short} = 27.8\ \mu s$ and $T_{long} = 301\ \mu s$ while the green one denotes a fit to a single exponential function, $I = A\exp(-T/T_1)$ with $T_1 = 54.8\ \mu s$. (Lower panel) Temperature dependence of a spin-spin relaxation time, T_2, for {Cu$_3$-Sb} crystal (green open inverse triangles), {Cu$_3$-As} crystal (black open squares) and {Cu$_3$-As}:NS (red open circles) at 7.63 T as well as for {Cu$_3$-As}:NS (blue open triangles) at 8.32 T. The solid lines are a fit to Eq. (2). Inset: Decay of the integrated Hahn echo area as a function of delay time (2τ) recorded for {Cu$_3$-As} crystal at T=1.50 K and H=7.63 T. The red solid line is a fit to a single exponential function $I = I_0\exp(-2\tau/T_2)$ with $T_2 = 696 \pm 30$ ns.

{Cu$_3$-As} crystal at the transition **1** as a function of the delay time 2τ. The echo intensity decay is well described by a single exponential function $I = I_0\exp(-2\tau/T_2)$, yielding a coherence time of $T_2 = 696 \pm 30$ ns at 1.50 K. Before proceeding, we stress that {Cu$_3$-As}:NS is free from structural distortions and disorders, as evidenced by no relaxation time

TABLE II: T_1 and T_2 of {Cu_3-X}(X=Sb,As) molecules under different environments measured at 1.50 K and 240 GHz. as-grown stands for {Cu_3-X}(X=Sb,As) crystals, deuterated for deuterated samples, NS(1) and NS(2) for {Cu_3-As} molecules enclosed in semiconducting nanoporous with two different concentrations, and finally Metal NS for {Cu_3-As} molecules impregnated in metallic nanoporous, respectively.

		{Cu_3-As}					{Cu_3-Sb}
	Field	as-grown	deuterated	NS(1)	NS(2)	Metal NS	as-grown
$T_1^{short}(\mu s)$	8.32 T	19.9 ± 2	22.3 ± 2	23.1 ± 3	24.6 ± 2	20.8 ± 2	19.3 ± 3
$T_1^{long}(\mu s)$	8.32 T	292 ± 20	265 ± 20	274 ± 30	237 ± 20	249 ± 20	285 ± 24
$T_2(ns)$	7.55 T	745 ± 35	971 ± 60	1190 ± 50	1066 ± 45	1016 ± 35	482 ± 34
	8.32 T	736 ± 25	705 ± 40	789 ± 30	873 ± 25	749 ± 30	557 ± 45

spreads[26].

At H=7.63 T and H=8.32 T most of the copper spins are polarized to the $|\frac{3}{2}; -\frac{3}{2}\rangle$ state so that single spin flips are suppressed. Thus, the transverse relaxation time at elevated temperature is dominated by a spin flip-flop process. For a quantitative description, the temperature dependence of $1/T_2$ is analyzed by a spin bath decoherence model[16];

$$\frac{1}{T_2} = A \sum_{m=1}^{7} W(m)P(m)P(m+1) + \Gamma_{res}, \tag{2}$$

where A is a temperature independent parameter and Γ_{res} is a temperature independent residual relaxation rate. Here, $P(m) = \exp(-E(m)/k_BT)/Z$ where Z is the partition function of the {Cu_3-X} spin system. $E(m)$ is read directly from the energy levels at H=7.63 T and H=8.32 T [See Fig. 2(b)]. $W(m)$ is the flip-flop transition probability for the m-th state with $\Delta m = \pm 1$. The experimental data are well fitted to Eq. (2). For the {Cu_3-As} crystal, we obtain the typical values of the leading term $W(1) = 0.38(1)\,\mu s^{-1}$ and the residual term $\Gamma_{res} = 0.70(8)\,\mu s^{-1}$, which amounts to $T_2^{res} = 1.4\ \mu s$. The {Cu_3-Sb} crystal shows a much steeper temperature dependence than the {Cu_3-As} one. Compared to the {Cu_3-As} crystal, {Cu_3-As}:NS exhibits the weaker temperature dependence. This is due to the almost absence of dipolar couplings to the fluctuating neighboring {Cu_3-As} spin clusters in NS. With increasing field from H=7.63 T to H=8.32 T, $1/T_2$ of {Cu_3-As}:NS tends to decrease due to enhanced polarization.

In order to investigate the intrinsic sources of spin decoherence we have measured the T_1 and T_2 relaxation times for samples with different symmetries and environments at 1.5 K: (i) as-grown {Cu_3-X} crystals, (ii) deuterated {Cu_3-As} crystal, (iii) {Cu_3-As}:NS with two different concentrations, and (iv) {Cu_3-As} impregnated in a metallic NS. Since the measured temperature is much smaller than the Zeeman energy at 8.32 T, the T_1 time will be governed by a single phonon process. Actually, we find no substantial sample dependence in the T_1 within errors. This suggests that the spin-lattice relaxation rate is hardly influenced by the distortions of peripheral organic ligands.

We next discuss possible mechanisms leading to the sample dependence of T_2. First, the coupling of electron spins to protons and ^{63,65}Cu (I=3/2) may provide an efficient decoherence path for a molecular magnet containing abundant protons[27]. Here, the protons and the Cu nuclear spins relaxed by spin-spin relaxation cause fluctuations of the hyperfine field at the observed electron spins. However, the nuclear spin contributions to decoherence tend to be largely suppressed at the high field at H=8.32 T[17]. Indeed, the deuterated {Cu_3-As} sample does not show a substantial increase of T_2. Moreover, the two {Cu_3-X}(X=As, Sb) crystals with the same nuclear isotopes exhibit the change of T_2 by 25 %. This indicates that the nuclear spins are not a serious decoherence source.

Second, the effect of intermolecular dipolar interactions is checked by confining the {Cu_3-X} molecule into NS[28,29]. An increase of T_2 is less than two times at 1.5 K. This might be due to fact that the total spin of the {Cu_3-X} molecule is as small as S=3/2 and shows that the intermolecular dipolar interactions do not provide the most significant decoherence channel although they are not negligible.

Lastly, we repeat the relaxation measurements by changing the conductivity of NS. The only slight reduction of T_2 (Table II) evidences that there are no substantial interactions between conducting electrons of a metallic NS and the core electron spins of the {Cu_3-X} molecule. This demonstrates that the {Cu_3-X} molecules can be incorporated into silicon nano-devices without causing a substantial spin decoherence.

It is remarkable that the relaxation times of {Cu_3-X}:NS are not much longer than those of the single crystal in spite of the isolation of the {Cu_3-X} molecules. We find no noticeable concentration dependence of the relaxation times. This implies that the {Cu_3-X} molecules are almost homogeneously dispersed into NS and rules out a formation of small multi-molecule assemblies within the NS. Besides, as described above, absorption of oxygen

is improbable.

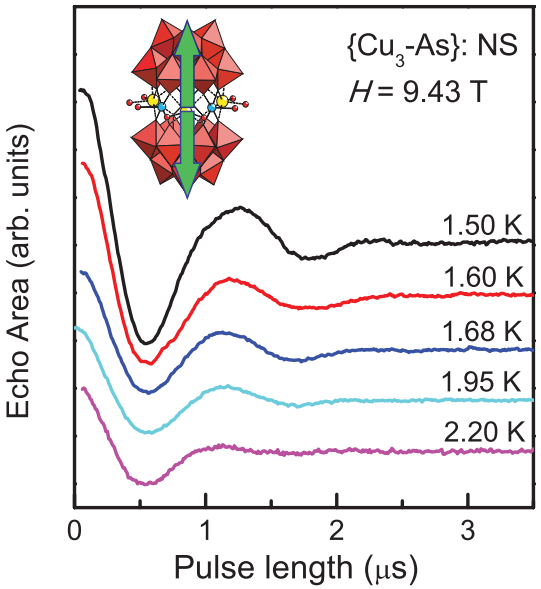

FIG. 4: Temperature dependence of Rabi oscillations obtained by recording the echo intensity as a function of nutation pulse length on {Cu_3-As}:NS at H=9.43 T.

All this strongly suggest that the AF triangle spin rings can have another effective decoherence route. We stress that {Cu_3-As} and {Cu_3-Sb} with different symmetries show an appreciable difference in T_2 (see Table II and the lower panel of Fig. 3). Since isosceles distortions are stronger in {Cu_3-Sb}, which shows a faster relaxation, a mixing degree of the two chiral states might be a key parameter. The chiral states can be mixed by structural distortions from an equilateral triangle and internal vibration modes (for example, an out-of-phase stretching vibration of the triangular clusters)[30]. This static distortion and dynamics spin-phonon coupling can be more dominant decoherence mechanisms for a spin triangle than the conventionally discussed ones. This tells us that we can improve a spin memory time through a molecule symmetry engineering.

To demonstrate a coherent manipulation of the electron spin in {Cu_3-As}:NS, we performed transient nutation experiments on the resonant transition **3**. After a nutation pulse of variable duration ν_{nut}, the longitudinal magnetization was indirectly detected by a two-pulse sequence (ν_{nut}-τ-$\pi/2$-τ-π-echo). For temperatures below 2.2 K at H=9.43 T we observe Rabi oscillations which correspond to coherent oscillation of the electron spin between the $|\frac{1}{2};-\frac{1}{2}\rangle$ and $|\frac{1}{2};\frac{1}{2}\rangle$ states of the $S^T = 1/2$ levels. As expected, the frequency and damping of the observed oscillations relies on temperature. This nutation experiment demonstrates

directly a realization of a NOT gate, which is one-qubit gate for quantum computation. The signal associated to the transient nutation of the electron spin has completely decayed within 3 μs. The decay time coincides with the transverse relaxation time (see Table II), implying that the dephasing of the Rabi oscillation is largely governed by the T_2 mechanism.

In conclusion, AF spin triangle $\{Cu_3\text{-}X\}$ molecules impregnated in nanoporous silicon create new avenues for a spin qubit methodology. A spin memory time reaches as long as $T_2 = 1066$ ns at 1.5 K. This together with the observation of Rabi oscillation demonstrates the microwave control of an electron spin of the hybrid material $\{Cu_3\text{-}X\}$:NS. The relaxation measurements in controlled environments suggest that spin decoherence is mainly governed by a new mechanism, involving transitions between states of equal spin but different chirality, and which depends on the molecular symmetry.

KYC acknowledges financial support from the Alexander-von-Humboldt Foundation and Korea NRF Grant (No. 2009-0093817 and 2010-0011325). Work was partially supported by DFG and NTH School Contacs in Nanosystems. The National High Magnetic Field Laboratory is supported by NSF Cooperative Agreement No. DMR-0654118, and by the State of Florida.

---

* kchoi@cau.ac.kr

[1] D. P. DiVincenzo, Science **270**, 255 (1995).

[2] M. N. Leuenberger and D. Loss, Nature **410**, 789 (2001).

[3] F. Meier, J. Levy, and D. Loss, Phys. Rev. Lett. **90**, 047901 (2003).

[4] F. Troiani *et al.*, Phys. Rev. Lett. **94**, 190501 (2005).

[5] W. Wersndorfer, Nat. Mater. **6**, 174 (2007).

[6] J. Lehmann *et al.*, Nature Nanotech. **2**, 312 (2007).

[7] A. Candini *et al.*, Phys. Rev. Lett. **104**, 037203 (2010).

[8] F. Luis *et al.*, Phys. Rev. Lett. **107**, 117203 (2011).

[9] J. Stolze and D. Suter, Quantum Computing (Wiley-VCH, Weinheim, 2004)

[10] Johan van Tol, G. W. Morley, S. Takahashi, D. R. McCamey, C. Boehme, M. E. Zvanut, Appl. Magn. Reson. **36**, 259 (2009).

[11] G. A. Timco *et al.*, Nat. Nanotechnol. **4**, 173 (2009).

[12] A. Ardavan *et al.*, Phys. Rev. Lett. **98**, 057201 (2007).

[13] G. Mitrikas *et al.*, Phys. Chem. Chem. Phys. **10**, 743-748 (2008).

[14] S. Bertaina *et al.*, Nature **453**, 203 (2008).

[15] C. Schlegel *et al.*, Phys. Rev. Lett. **101**, 147203 (2008).

[16] S. Takahashi *et al.*, Phys. Rev. Lett. **102**, 087603 (2009).

[17] S. Takahashi *et al.*, Nature **476**, 76 (2011).

[18] D. P. DiVincenzo, Fortschr. Phys. **9-11**, 771-783 (2000).

[19] S. Carretta *et al.*, Phys. Rev. B **76**, 024408 (2007).

[20] K.-Y. Choi *et al.*, Phys. Rev. Lett. **96**, 107202 (2006).

[21] K.-Y. Choi *et al.*, Phys. Rev. B **77**, 024406 (2008)

[22] U. Kortz *et al.*, Inorg. Chem. **40**, 4742 (2001).

[23] P. Kumar *et al.*, J. Appl. Phys. **103**, 024303-024306 (2008).

[24] H. Nojiri, K.-Y. Choi, and N. Kitamura, J. Magn. Magn. Mater. **310**, 1468 (2007).

[25] J. van Tol, L. C. Brunel, and R. J. Wylde, Rev. Sci. Instrum. **76**, 074101 (2005).

[26] M. F. Collins and O. A. Petrenko, Can. J. Phys. **75**, 605 (1997).

[27] N. V. Prokof'ev and P. C. E. Stamp, Rep. Prog. Phys. **63**, 669 (2000).

[28] P. C. E. Stamp and I. S. Tupitsyn, Phys. Rev. B **69**, 014401 (2004).

[29] A. Morello, P. C. E. Stamp and I. S. Tupitsyn, Phys. Rev. Lett. **97**, 207206 (2006).

[30] H. Nakano and S. Miyashita, J. Phys. Soc. Jpn. **71**, 2580 (2002).